

Use of Fixed-Range Noise Radar for Moving-Vehicle Identification

Eric K. Walton

*The Ohio State University
Columbus, OH 43212-1191
Phone: (614) 292-7981
e-mail: walton.1@osu.edu*

Abstract

The Ohio State University ElectroScience Laboratory has built a radar that transmits ultra wideband (UWB) random noise. The received signal is cross correlated with a fixed delay version of the transmitted signal. This produces a radar detection ring at a fixed distance from the radar. As a vehicle or person moves through the detection ring, the range profile and the time dynamics of the moving person/vehicle are traced out. This permits identification, as well as detection of the moving object. We will present a description of the system and show example data. Example signatures will be shown and discussed. The potential for an unattended ground sensor in the foliage penetration and target classification mode will be discussed.

Introduction

The Ohio State University ElectroScience Laboratory has built a radar that transmits UWB random electromagnetic (EM) noise. Such a spread-spectrum waveform is very difficult to detect because it is a low probability of intercept (LPI) signal. It is also unlikely to interfere with other users of the operational frequency band, and it is unlikely that other signals in the band will “jam” its operation; as with all such spread-spectrum systems, interference appears as spectrally spread-out noise after processing.

Radar System

In the construction of such a radar, a copy of the transmitted signal is delayed and then cross correlated with the received signals using a mixer and a low-pass filter. The resultant cross-correlation function is directly proportional to the convolution of the radar target and the radar

system impulse response. After calibration, one can extract the radar target impulse response. This response can be Fourier transformed to the frequency domain, providing a UWB coherent measure of the radar scattering. Thus we have a fully coherent radar that can provide target scattering amplitude and phase. A block diagram of this radar system is given in figure 1.

One way of describing this radar system is to break up the input signal into a Fourier series, as shown in figure 2.

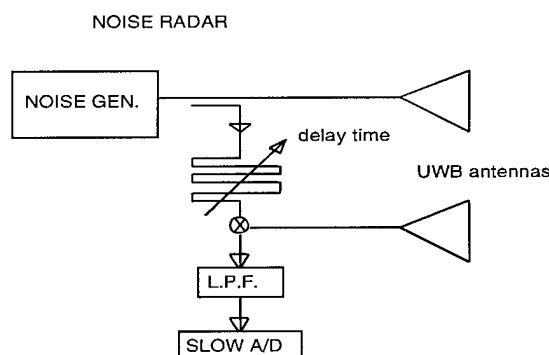
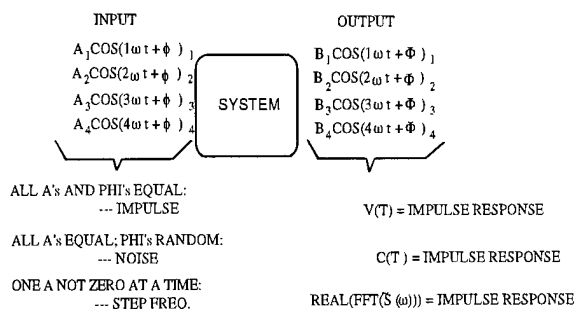


Figure 1. Block diagram of noise radar.



COMPARISON OF IMPULSE, NOISE AND STEP FREQUENCY RADARS

Figure 2. Fourier series representation.

100-101000-100000

AA I-99-04-0511

In this figure, we show that the only difference between radars of different waveforms is in the way the waveform is synthesized. Fixed phases for the individual frequency domain components produce an impulse, and random phases produce noise of equal bandwidth. One signal at a time produces a step frequency radar. Following this analysis approach, it can be shown that multi-frequency, impulse and noise radars have the same post processing signal-to-noise ratio (S/N) (if they have the same bandwidth).

In the system that we will discuss in this paper, two 1- to 700-MHz 30-dB amplifiers were fed by a 50 Ω matched load to give approximately 1 mW of noise power. This frequency band is useful for foliage penetration, as well as for building wall penetration, and we plan to use it in this mode in the future. The delay line was not variable, but was fixed to 50 or 75 feet of coaxial line. The low-pass filter was a multi-stage unit, with a 1-MHz RF filter, followed by an active stage with a 10-Hz cut-off.

The antennas were a pair of 8-ft.-long trapezoidal rhombics mounted side by side with vertical polarization. The system was set up in the open field behind the laboratory building, and various vehicles and walking people were moved through the range gate.

Experimental Data

We start by showing the data for one subject, to be referred to as "E.K.W.," walking toward and away from the radar so that he passes through the range gate. As he walks through the range gate, he traces out his radar impulse response, except that he is moving his legs and arms during the passage through the range gate. For this reason, I call these response profiles "range profiles" rather than "impulse responses." An example plot for E.K.W. is shown in figure 3.

The data shown in figure 3 include the entire experiment, where the person walked through the range gate several times. If we extract two individual passes, the resulting set of range profiles can be overlaid and compared. The results for E.K.W. are shown in figure 4. We show similar data for "S.U.G." in figure 5.

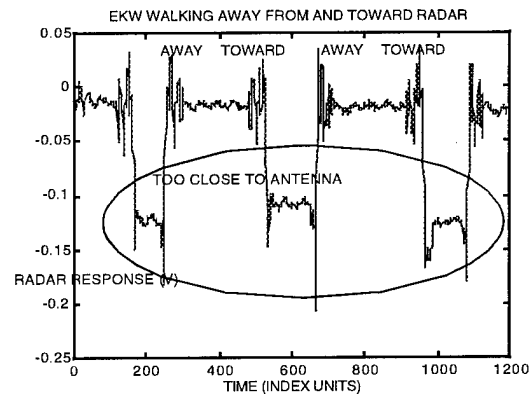


Figure 3. Range profile for E.K.W. walking through the radar range gate.

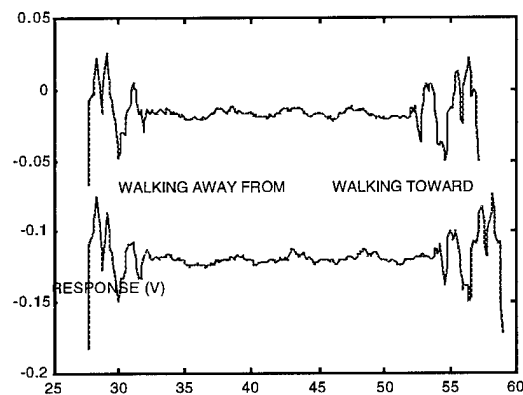


Figure 4. Range profiles for E.K.W.

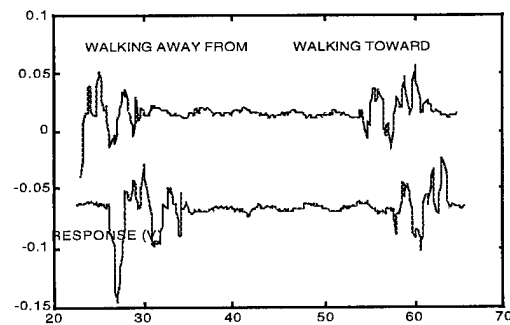


Figure 5. Range profiles for S.U.G.

Note that the response for walking toward the radar is the mirror image of the response for walking away. Also note that the range profile for each walking person is similar.

These data were obtained in an open field, using only 7 mW of total transmitted noise power. The scattered signal from the walking person was estimated to be minus 50 dBm. A spectrum analyzer showed a number of interfering radio transmitters in the area (FM, TV, cellular, etc.). The strongest (at 65 MHz) had a received signal level of minus 15 dBm. Thus these walking-person results were obtained when the received scattered signal was on the order of 35 dB below that of the received signal from at least one of the interfering sources. This is a demonstration of the signal processing power of the noise correlation system (mixer and filter). We claim that the signal processing system gives a signal enhancement of the ratio of the transmitted signal bandwidth to the low pass filter bandwidth. In this case, we have 0.6×10^9 to 10, or 78 dB signal processing gain due to the spread-spectrum-type processing.

We can calibrate the system by pulling an 18-in. sphere on a plastic sled through the range gate using a string. (The details are beyond the scope of this short paper.) We also drove an automobile through the range gate. This gives us a range profile (and impulse response after calibration) for the automobile. The range profile for the moving automobile is shown in figure 6. (The ripple is due to active LP filter oscillation.)

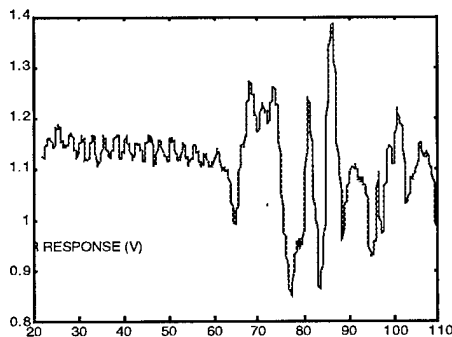


Figure 6. Range profile for automobile.

We have measured a larger number of automobile types and plan to develop target classification techniques based on the resulting data-base.

Data Analysis

It can be seen that this simple noise radar can be used to form a "radar trip wire" or fixed range gate sector where any vehicle or person will cause a response. We believe that it can also be used to identify or classify these various targets. Clearly the walking person or group of people will have different dynamic characteristics (walking movements) and different range profile characteristics than an automobile, truck or tracked vehicle (or even a deer or cow). Note, however, that without an estimate of the speed of the target, we cannot calibrate our range profile in units of distance. One can build the noise radar to have several concentric range gates by using multi-tapped delay lines. This permits parallel processing and detection of targets passing through the range gates, and permits an estimate of speed. Unfortunately, the direction of motion of the target must be known to fully exploit such a concept. One might use crossed-loop, direction-of-arrival detection so that radial motion of the target can be determined. More work on this topic is required.

Conclusions

We have discussed and demonstrated the development and operation of a noise radar. We have shown that it is possible to extract range profiles (including time dynamics) of targets such as walking people and moving vehicles as they pass through the range gate. We believe that these data provide a rich environment for development of features in a target classification system.

We have operated this radar in the presence of received signals from other radio transmitters where the received total power from the interference transmitters was 40 dB stronger than the scattered signal from the radar target, but no effect can be seen other than a small degradation in the overall signal to noise ratio on the target.

We plan to operate this radar in the foliage penetration mode in the near future.

Ultra-Wideband Foliage and Ground-Penetrating Radar Experiments

Karl A. Kappra, Francis Le, Lam Nguyen, Tuan Ton, Matthew Bennett

U.S. Army Research Laboratory

Adelphi, MD 20783-1197

Phone: (301) 394-0848

e-mail: kkappra@arl.mil

Abstract

The Army Research Laboratory (ARL) is executing technology development programs to evaluate the potential use of ultra-wideband synthetic aperture radar (UWB SAR) technology to detect and classify targets concealed by foliage and subsurface targets. Under these programs, a very capable, 1-GHz-bandwidth, low-frequency, fully polarimetric, UWB SAR instrumentation system was developed to collect the data needed to support the penetrating radar studies. This paper describes two foliage and ground penetrating radar experiments conducted with this radar.

Introduction

The radar was integrated onto a 150-ft-high boomlift platform in 1995 and was thus named the BoomSAR. The BoomSAR system has collected data at Aberdeen Proving Ground (APG), MD, and Yuma Proving Ground (YPG), AZ. The APG experiments focused on supporting the foliage-penetrating radar investigations, while the YPG experiment focused on supporting the ground-penetrating radar program objectives. This paper describes these experiments and provides SAR imagery that gives an indication of possible target/clutter discrimination techniques.

BoomSAR System

The BoomSAR has several important features that support the foliage-penetration (FOPEN) and ground-penetration (GPEN) radar investigations: It can travel to areas of differing soil/clutter environments (the obvious mobility advantage); it can move while elevated to generate extended synthetic apertures; the telescoping arms are articulated for generating two-dimensional apertures for three-dimensional image formation; and it can collect data at different depression angles and at geometries similar to that which may be seen by an airborne system. The BoomSAR permits the evaluation of most of the issues associated with an airborne system, but in a more precisely controlled, repeatable environment.¹ While collecting the radar data, the BoomSAR system drives at a speed of approximately 1

km/hour, creating the desired synthetic aperture. Figure 1 shows the BoomSAR system on the Perryman Test highway at Aberdeen Proving Ground. This road was ideal for accommodating the extended 18-ft wheel base of the 27-ton boom-lift.

BoomSAR Components

The testbed consists of several major subsystems, as depicted in the block diagram in figure 2. These components are modular, which simplifies the exchange and evaluation of alternative approaches. The testbed radar subsystems consist of transverse electromagnetic (TEM) horn antennas, Power Spectra 2-MW peak power impulse transmitters, Tektronix 8-bit analog-to-digital (A/D) converters, Mercury i860 processors, six magneto-optical disks for data-storage, a timing and control assembly, a Geotronics 4000 position location subsystem for tracking the antenna location, and a Sparc 2E, which acts as the operator interface. Much of the system operation is controlled by software and programmable logic, allowing for a relatively simple path of modification or upgrade.

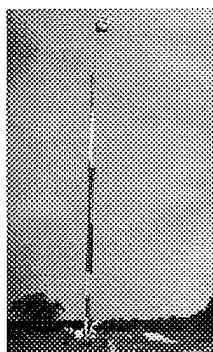


Figure 1. BoomSAR.

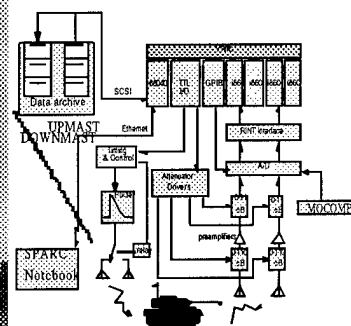


Figure 2. BoomSAR block diagram.

The BoomSAR uses an impulse waveform with spectral response extending from 50 MHz to over 1 GHz. This 1-GHz bandwidth, which is directly digitized on receive, gives a measured 5-in. resolution in the range dimension. High resolution in the cross-range dimension is achieved with the use of SAR techniques to process those returns to achieve resolution as small as 6 in. To obtain the required polarimetric data, we transmit pulses sequentially, either with linear horizontal or vertical polarization, and simultaneously

receive co- and cross-polarized data to produce vertical transmit, vertical receive (VV) polarization and horizontal transmit, horizontal receive (HH), HV, and VH data.² The radar currently operates at a pulse repetition frequency rate of 700 Hz.

Processor/Data Storage Subsystem

The radar processor is a Motorola 68040-based VME chassis, running under VxWorks, with two separate groups of six i860 array processors running under the Mercury Computer operating system. A SCSI interface is used for recording the pre-processed or interleaved data from each transmit polarization channel on separate 1.3-GB rewriteable magneto-optical disk drives. Typically 2.5 km of aperture is recorded without having to stop the BoomSAR to flip over the disks.

Aberdeen Proving Ground Experiment

The 5-km length of the Perryman Test Highway in Aberdeen Proving Ground allowed large volumes of target and clutter data to be collected to support the foliage-penetrating radar investigations, while also permitting subsurface targets to be placed in the scene. Another attractive feature of the test area was that vehicle test tracks were cut into the foliated areas providing ideal and unique opportunities to set up and collect data on vehicles and canonical targets in the clear, and behind one or more tree canopies viewed from multiple aspect angles. Figure 3 is a photograph taken from the boom-lift platform at its full 150-ft extension. APG foliage consists of a mix of deciduous trees with tall brush in the cleared area.

Figure 4 is schematic of the target scenario on the east side of the Test Highway. In one data collection run, data were recorded for the full 2-km length. Each of the 14 vehicles (depicted as rectangles in figure 4) in the scene was rotated by 15° for each of the subsequent data collection runs to provide multiple look angles (target realizations) for each of the vehicles. This is important for providing a statistically significant data set so that we can evaluate the robustness of various target discrimination algorithms.

Extensive analysis of the radar data from the Aberdeen and Yuma experiments has led to the definition of processing steps that have improved the radar signal-to-noise ratio. For example, the boom-lift platform evidently induced a low-frequency resonance, which is apparent in the data sets. However, this resonance is consistent enough that we can effectively remove it by applying a filter developed from a sliding average of the data — this processing step is referred to as self-interference removal (SIR). Figure 5 is a SAR image of

data collected at APG. The processing that has been performed on the image in figure 5 includes motion compensation, background subtraction, Hilbert transform, and mosaic back-projection focusing. This SAR image was generated using 7400 aperture positions (740 m) to form an image 230 x 200 m. The mosaic image formation routine allows for a constant 90° integration angle ($\pm 5^\circ$) throughout the image.³

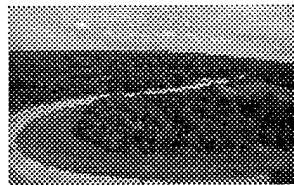


Figure 3. View from boom.

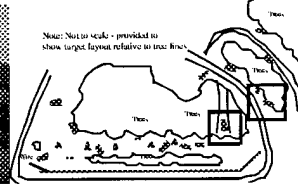


Figure 4. Target scenario.

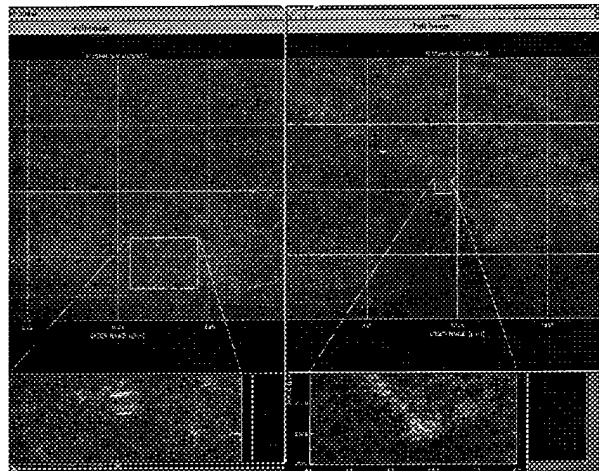


Figure 5. SAR image from APG.

Yuma Proving Ground Experiment

The Yuma experiment was conducted in January/February 1996. With support from YPG and MIT/Lincoln Laboratory, ARL established a subsurface target test site at YPG known as the Steel Crater Test Area. Because the objective of the customer-funded Steel Crater Program was to investigate the potential of an airborne ground-penetrating radar, a tremendous variety of targets were placed in the Steel Crater area. These targets support the evaluation of the use of UWB SAR technology in stand-off sensors to support military operations, intelligence gathering, treaty verification, environmental clean up, and the commercial utility industry.

The Steel Crater site is unique in that half the area is part of the Phillips Drop Zone area, in which the soil has been turned over to a depth of a couple of feet and is free of vegetation—an almost homogeneous soil layer. This feature allowed us to conduct electromagnetic wave

propagation studies in a realistic but relatively easily definable soil. Targets were also buried in the naturally occurring clutter areas. Figure 7 shows the entire Steel Crater test area, and table 1 describes the representative targets in the test site. The BoomSAR collected data from Boom Road, Corral Road, and the dirt road on the north edge of the test site.

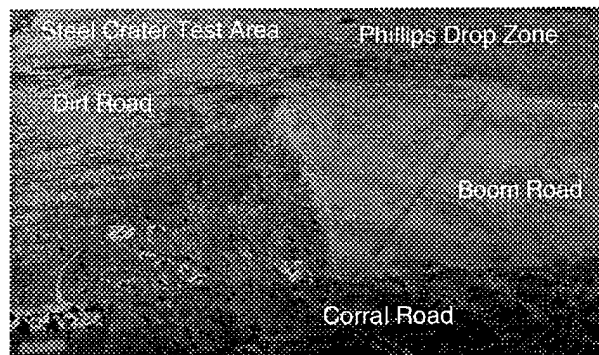


Figure 7. YPG test site.

Target	Class of Target
Wires: various gauges, fiber optic	Underground structures: comm wires, power cables
Horizontal pipes: plastic and metal	Underground facilities: water, sewage, etc.
Vertical pipes	Underground facilities: ventilation shafts
55-gallon drums	Environmental waste
Storage containers	Buried arms caches
Tracked and wheeled vehicles	Buried/hull defilade
Mines: metal and plastic	Anti-tank & anti-personnel
Unexploded ordnance	Environmental waste

Table 1. Targets in test site.

The objectives of the experiment required a comprehensive soil characterization.⁴ This soil analysis permits using the collected data to verify the accuracy of electromagnetic models. Then these models can be used to extrapolate performance of the radar in other soil conditions.

Figure 8 is the schematic layout of the anti-tank and anti-personnel minefield. Figure 9 is the full-band SAR imagery of the minefield. The high resolution of the BoomSAR imagery allows the small Valmara 69 anti-personnel mines to be visible.

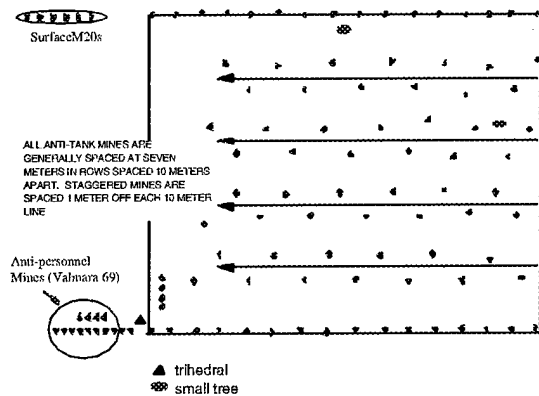


Figure 8. Schematic layout of minefield at YPG.

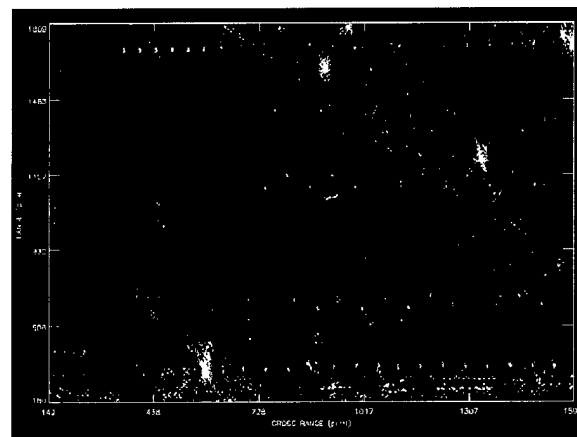


Figure 9. SAR image of minefield at YPG.

Although the instrumentation-grade BoomSAR system encompasses 1 GHz of low-frequency bandwidth, a military fielded or commercially produced foliage- or ground-penetrating radar may not need the entire extended frequency coverage. However, with this bandwidth, more investigations can be conducted to determine the optimal frequency coverage to detect particular targets.

A method of moments (MOM) model was used to analyze where the resonant frequency (maximum radar cross-section) for an M20 mine occurs. With this information, the full-band data were sub-banded from 400 to 1000 MHz and from 300 to 500 MHz, as shown in figures 10 (a) and (b), respectively. The subsurface M20 mines are not visible in the higher sub-band because the data used were above the resonant region of this 14-in.-diameter metal mine. On the other hand, the 4-in.-diameter anti-personnel mines are clearly visible, because this sub-band is closer to the resonance region of the Valmara 69 mines. Likewise, the M20 mines are quite apparent in the lower sub-band, which is in the resonant region of this size mine.

This kind of analysis is an indication of the value of the BoomSAR system for providing data that allow the optimal frequency to be determined for detecting particular targets of interest.

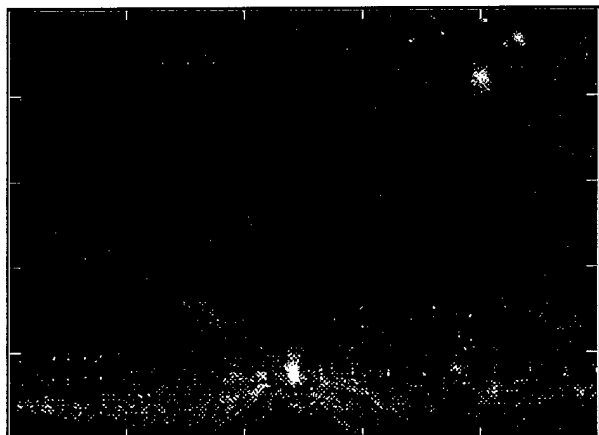


Figure 10a. 400-1000 MHz sub-banded image of minefield. Note: increased contrast from smaller Valmara 69 mines.



Figure 10b. 300-500 MHz sub-banded image of minefield. Note: greater contrast from larger M20 mines. Also note lack of contrast from Valmaras because data processed outside their resonance region.

Conclusion

The ARL BoomSAR is a state-of-the-art instrumentation radar that can provide the high-resolution, high-sensitivity data needed to conduct foliage- and ground-penetrating radar investigations. This system complements the existing airborne low-frequency SAR systems, because it provides the ability to collect reasonable amounts of data in a very controlled environment with the same depression angles as the airborne sensors. The unique features of the low-frequency data and the resultant imagery of the data collected with the BoomSAR indicate that there is potential for low-frequency UWB radar to detect targets embedded in foliage and subsurface targets. More work

is needed to develop effective target/clutter discrimination techniques to ensure that a reasonable low false-alarm rate could be realized.

Future Work

A new TEM horn antenna has been built that extends the frequency coverage of the BoomSAR system from 25 MHz to over 1 GHz. Horizontal polarization data have been collected with the new antenna at the Perryman Test Highway in APG. The objective of lowering the frequency coverage was to determine whether there will be lower backscatter return from the clutter environment and higher return from man-made objects in the low VHF region. Data were not available at the time of publication of this paper.

One of the near-future upgrades for the BoomSAR includes the integration of a Litton Inertial Navigation System (INS), which will be used with the Geotronics 4000 to provide a 50-Hz update rate for the motion compensation information archived with the radar data. Other off-the-shelf analog-to-digital (A/D) converters are also being considered for integration and evaluation in the BoomSAR system.

Acknowledgments

The authors would like to acknowledge Marc Ressler, John Clark, Jeff Sichina, Mosh Qaadri, Lynn Happ and Keith Sturgess whose contributions were critical to the successful execution of these experiments.

References

1. K. Kappra, L. Happ, F. Le, L. Nguyen, "ARL Foliage and Ground Penetrating Radar Experiments and Results (U)," Tri-Service Radar Symposium (June 1996). (SECRET)
2. M. Ressler, "The Army Research Laboratory Ultra-wideband BoomSAR," IGARSS '96, Volume 3, pp. 1886-1888.
3. J. McCorkle and M. Rofheart, "An Order $N^2 \log(N)$ Radon Transform for SAR," SEDD Symposium (January 1997).
4. M. Collins, R. Kuehl, D. Heuberger, and J. Kurtz, "Soil Properties at the YPG as Related to GPR," unpublished (December 1995).

INTERNET DOCUMENT INFORMATION FORM

A . Report Title: Use of Fixed-Range Noise Radar for Moving-Vehicle Identification

B. DATE Report Downloaded From the Internet 1/5/99

C. Report's Point of Contact: (Name, Organization, Address, Office Symbol, & Ph #): The Ohio State University
Eric K. Walton (614) 292-7981
Columbus, OH 43212-1191

D. Currently Applicable Classification Level: Unclassified

E. Distribution Statement A: Approved for Public Release

F. The foregoing information was compiled and provided by:
DTIC-OCA, Initials: VM_ **Preparation Date:** 1/5/99__

The foregoing information should exactly correspond to the Title, Report Number, and the Date on the accompanying report document. If there are mismatches, or other questions, contact the above OCA Representative for resolution.